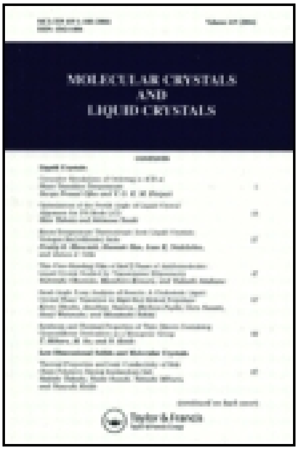

Molecular Crystals and Liquid Crystals
Publication details, including instructions for authors and subscription information:
http://www.tandfonline.com/loi/gmcl16

Evidence for Acoustic Streaming in the Nematic Acousto-Optic Effect

C. F. Hayes [a]

[a] Dept. of Physics and Astronomy, University of Hawaii, Honolulu, Hawaii, 96822, U.S.A

Version of record first published: 20 Apr 2011.

To cite this article: C. F. Hayes (1980): Evidence for Acoustic Streaming in the Nematic Acousto-Optic Effect, Molecular Crystals and Liquid Crystals, 59:3-4, 317-328

To link to this article: http://dx.doi.org/10.1080/00268948008071431

Mol. Cryst. Liq. Cryst., 1980, Vol. 59, pp. 317–328
0026-8941/80/5903-0317$04.50/0

Evidence for Acoustic Streaming in the Nematic Acousto-Optic Effect

C. F. HAYES
Dept. of Physics and Astronomy, University of Hawaii, Honolulu, Hawaii 96822, U.S.A.

(*Received August 1, 1979; in final form September 29, 1979*)

In an effort to understand the acousto-optic effect in nematic liquid crystals both the velocity and the flow pattern in a disc-shaped sample of ordinary fluid have been experimentally determined. The hydrodynamic equations for an acoustically excited fluid disc are solved to second order and shown to agree with the experimental velocity measurements of the ordinary fluid disc as well as the observed light transmission pattern for a nematic disc.

I INTRODUCTION

The acousto-optic effect in liquid crystals was discovered by Fredericks and Zolin[1] in 1936. They excited a nematic liquid crystal cell with tuning forks of 200 to 600 Hz while observing the light transmitted through the cell which was placed between crossed polarizers. Differential acoustic absorption,[2] transverse second-order stress,[3] the presence of cybotactic groups,[4] the piezoelectric effect,[5] and anisotropy of acoustic velocity[9] have all been proposed mechanisms for the effect. Prior to 1976 it was assumed in both experimental and theoretical research articles that a threshold of acoustic intensity is required. In 1976 four groups: Sripaipan, Hayes, and Fang,[6] Candau, Peters, and Nagai,[7] Miyano, and Shen,[8] and Dion, and DeForest[9] reported that there is in fact no threshold for the effect. Mechanisms other than streaming require some special property of a liquid crystal for the effect. Acoustic streaming occurs in any viscous liquid and in a liquid crystal results in optical effects. The streaming theory has been extended by Hayes[10] in 1978 to include the simultaneous effect of an electric field. Again the streaming model successfully explains the experimental results.

Even so, streaming is not accepted universally as the mechanism.[11,12] The evidence needed, it seems, is direct observation of the flow in the cell along with a detailed theory which describes both the speed of flow and flow pattern. In Section II we present such a theory and we solve the hydrodynamic equations to second order to find both the flow speed and flow pattern. In Section III, experimental confirmation of the predictions for an ordinary liquid is presented. Should such flows occur in a nematic the director would be affected and the transmission pattern for light traveling through a nematic cell placed between crossed polarizers can be predicted. A series of photomicrographs of a nematic is also given in Section III showing agreement with the expected pattern. In Section IV conclusions are given.

II THEORY

The problem to be solved concerns a disc shaped liquid which is confined between two solid planes and is radially open to the air. One can produce such a system by placing a drop of liquid on a microscope slide and covering the drop with a second slide. The thickness of the disc is determined by a spacer used to separate the slides. An acoustic wave is directed along the normal to the glass surface. We will assume one plane oscillates along the symmetry axis of the disc. We choose a cylindrical coordinate system with the z axis along the symmetry axis of the disc. The plane boundaries are located at $z = +H/2$ and $-H/2$ with the radial boundary at $r = R$.

We seek a solution of the Navier–Stokes and mass continuity equations which satisfies the appropriate boundary conditions. We assume the system remains in thermal equilibrium. The equations are respectively:

$$\rho_0\left[\frac{\partial \mathbf{v}}{\partial t} + (\mathbf{v}\cdot\nabla)\mathbf{v}\right] = -c^2\nabla\rho + \eta\nabla^2\mathbf{v} + (\zeta + \tfrac{1}{3}\eta)\nabla(\nabla\cdot\mathbf{v}) \tag{1}$$

$$\frac{\partial \rho'}{\partial t} + \nabla\cdot(\rho'\mathbf{v}) = 0 \tag{2}$$

where ρ' is the fluid density; v, the fluid velocity; c, the acoustic speed; η, the shear viscosity and ζ, the bulk viscosity. The zero subscript on ρ_0 refers to the equilibrium value of density without the presence of the acoustic wave. We take ρ to be the deviation from equilibrium: $\rho = \rho' - \rho_0$.

Assuming the time dependence to be $\exp(i\omega t)$, Eq. (1) and (2), taken to first order in the hydrodynamic variables, may be combined giving:

$$A_0\nabla^2\rho = \rho \tag{3}$$

where

$$A_0 = -\frac{i(\zeta + \frac{4}{3}\eta)}{\omega\rho_0} - \frac{c^2}{\omega^2} \tag{4}$$

We take as the form for the solution of Eq. (4):

$$\rho = \sum_n [A_{1n} J_0(k_n r) e^{k_n'' z} + A_{2n} J_0(k_n r) e^{-k_n'' z}] e^{i\omega t} \tag{5}$$

where

$$k_n^2 = k_n''^2 - \frac{1}{A_0} \tag{6}$$

To facilitate finding the velocity solutions we define two velocity potentials ϕ and ψ.

$$v_r = \frac{\partial \phi}{\partial r} + \frac{\partial \psi}{\partial z} \tag{7}$$

$$v_z = \frac{\partial \phi}{\partial z} - \frac{1}{r}\frac{\partial}{\partial r}(r4) \tag{8}$$

We therefore have

$$\nabla \cdot \mathbf{v} = \nabla^2 \phi \tag{9}$$

So from (2) and (3)

$$\phi = -\frac{i\omega A_0 \rho}{\rho_0} \tag{10}$$

Equations (1)–(8) may now be combined to give the surprisingly simple equation:

$$\frac{\eta}{i\omega\rho_0} \nabla^2 \xi = \xi \tag{11}$$

where

$$\xi = \frac{1}{r}\,\frac{\partial}{\partial r}(r\psi) \tag{12}$$

We find therefore

$$\xi = \sum_n [A_{3n} J_0(k_n r) e^{k_n' z} + A_{4n} J_0(k_n r) e^{-k_n' z}] e^{i\omega t} \tag{13}$$

where

$$k_n^2 = k_n'^2 - \frac{i\omega\rho_0}{\eta} \tag{14}$$

These solutions for ψ and ξ may be incorporated into Eqs. (7), (8), (10), and (12) to provide the velocity solution in terms of the coefficients, A_{in}. The coefficients in turn can be obtained from the boundary conditions:

We assume a non-slip condition at $z = +H/2$ and $-H/2$ and take $v_r = 0$ there. We take $\rho = 0$ at the radial boundary $r = R$. The acoustic wave causes the boundary at $z = -H/2$ to have $v_z = A\exp(-i\omega t)$. Since for our experiment the ratio of H to the acoustic wavelength is 0.055 we assume the second plane to also have this boundary condition. We will discuss the appropriativeness of this approximation later. From these boundary conditions we find

$$A_{1n} = -A_{2n} = \frac{-2\rho_0 k_n' A}{i\omega A_0 k_n'' \alpha_n J_1(\alpha_n)(2k_n' - k_n^2 H)} \tag{15}$$

$$A_{3n} = A_{4n} = \frac{2k^2 HA}{\alpha_n J_1(\alpha_n)(2k_n' - k_n^2 H)e^{k_n' H/2}} \tag{16}$$

For the system we wish to test experimentally $k_n' \gg k_n^2$H and k_2''H $\ll 1$. By analyzing the amplitudes of the modes in the non-viscous case we find the $n = 0$ mode predominates for small disc radii ($R < 0.383\lambda$). With these approximations we find the real components of the fluid velocity are

$$v_z = \frac{2AJ_0(k_0 r)\cos\omega t}{\alpha_0 J_1(\alpha_0)} \tag{17}$$

$$v_r = \frac{Ak_0}{\alpha_0 J_1(\alpha_0)}\{-2z + H[e^{R_e k_0'(z-H/2)}\cos[\mathrm{Im}k_0'(z - H/2) + \omega t] \tag{18}$$

$$- e^{R_e k_0'(z+H/2)}\cos[\mathrm{Im}k_0'(z + H/2) + \omega t]]\} \times J_1(k_0 r)$$

where $\alpha_0 = k_0 R = 2.405$, i.e. in general $J_0(\alpha_n) = 0$. Comparison of Eq. (17) with the assumed boundary condition $v_z = A\exp(-i\omega t)$ shows our approximation of dropping all but the zero order terms amounts to assuming there is a bowing of the plane fluid boundaries.

It is of interest to compare the amplitude of oscillation of the plane disc boundary with that of the radial boundary. We make this comparison by setting $r = R$ in v_r, Eq. (18), and by using the experimental values for our sample: $H = 0.032$ cm, $Re\, k_0' = \mathrm{Im}\, k_0' = 1{,}112$ cm, and $R = 0.22$ cm for mode $n = 0$ resonance. The resulting velocity ratio, v_R/A, is plotted as a function of z in Figure 1. Since the motion is harmonic this velocity ratio is also the ratio of the amplitude at the radial boundary to that at the plane boundary. The largest value for the ratio is approximately 0.14. Therefore, the plane disc boundary moves with an amplitude of over seven times that of the radial boundary. Nevertheless we will find as we proceed to second order that the major streaming in the bulk of the disc is radial.

So far we have obtained a solution by retaining only the linear terms in Eq. (1). The solutions we have obtained vary sinusoidally in time. Therefore

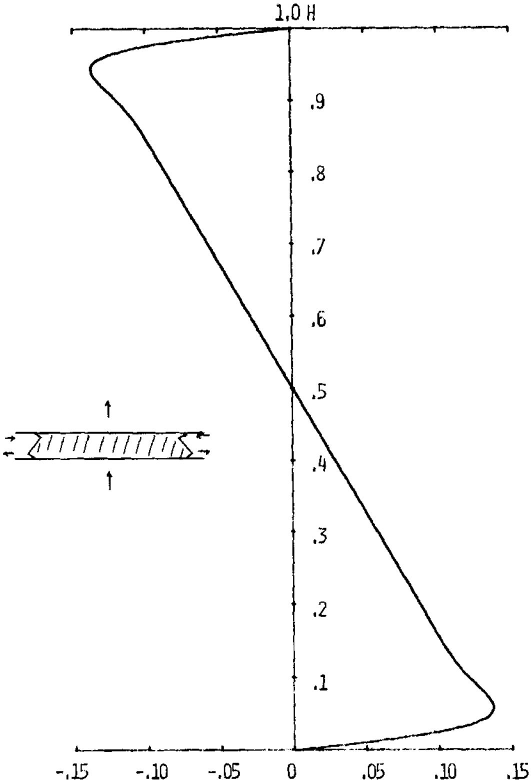

FIGURE 1 The velocity ratio, V_R/A, as a function of distance along the symmetry axis of the disc. The disc thickness is H. The velocity ratio is also the ratio of radial boundary oscillation amplitude to that of the plane.

the term $\rho_0(v \cdot \nabla)v$ will have a factor $\cos^2 \omega t$. Using the identity $\cos^2 \omega t = (1 + \cos 2\omega t)/2$ we see that taking the time average of Eq. (1) results in a non-zero static value of the hydrodynamic variables. For the velocity the phenomenon is called acoustic streaming. Invoking the previous approximations used for obtaining Eqs. (17) and (18) we find that we may identify ∇^4 with $\partial^4/\partial z^4$. Using the subscript 2 to denote this static addition to the hydrodynamic variables we find the contributions from ϕ_2 may be omitted and ψ_2 is given by:

$$\psi_2 = \frac{\rho A^2 k_0^3 J_1(k_0 r)}{2\eta\alpha_0^2 J_1(\alpha_0)} \cdot \frac{\partial J_1(k_0 r)}{\partial(k_0 r)} \left\{ - \frac{z}{4(R_e k_0')^3} \right.$$

$$\left. x[e^a(\cos a - \sin a) + e^{-b}(\cos b + \sin b)] + c_1 z^3 + c_2 z^3 + c_3 z + c_4 \right\} \quad (19)$$

where

$$a = \text{Re } k_0'(z - H/2) \tag{20}$$

$$b = \text{Re } k_0'(z + H/2) \tag{21}$$

The values of the constants C_i may be found using the boundary conditions which require that v_{2r} and v_{2z} are zero for $z = +H/2$. Finally, we obtain explicit relations for v_{2r} and v_{2z}:

$$v_{2r} = -\frac{\rho A^2 k_0^3 H J_1(k_0 r)}{\eta \alpha_0^2 J_1^2(\alpha_0)} \cdot \frac{\partial J_1(k_0 r)}{\partial(k_0 r)} \left\{ \frac{z}{2(\text{Re } k_0')^2} [e^a \sin a + e^{-b} \sin b] - \frac{3z^2}{2(\text{Re } k_0')^3 H^2} + \frac{3}{8(\text{Re } k_0')^3} \right\} \tag{22}$$

$$v_{2z} = -\frac{\rho A^2 k_0^3}{2\eta \alpha_0^2 J_1^2(\alpha_0)} \frac{1}{r} \frac{\partial}{\partial r} \left(r J_1(k_0 r) \frac{\partial J_1(k_0 r)}{\partial(k_0 r)} \right) \times \left\{ -\frac{z}{4(\text{Re } k_0')^3} \left[e^a(\cos a - \sin a) + e^{-b}(\cos b + \sin b) \right] + \frac{3z}{8(\text{Re } k_0')^3} - \frac{z^3}{2(\text{Re } k_0')^3 H^2} \right\} \tag{23}$$

Equations (22) and (23) specify the flow pattern shown in Figure 2–I. The pattern resembles the situation which would arise from standing waves set up by a radially excited acoustic wave. The ratio of H/R is much smaller than depicted in the diagram. One might have expected a flow as shown in Figure 2–II since the imposed acoustic wave is directed from $z = -H/2$ to $+H/2$. The dashed line in each flow loop shows the director tilt that would be induced by such a flow in a homeotropically aligned nematic crystal. The dotted line shows the director orientation without a flow.

III EXPERIMENT

A Velocity measurement

We are interested in the magnitude of acoustically excited flow in nematic liquid crystals. However, since the nematic liquid crystals strongly scatter light we have used a transparent vegetable oil doped with small opaque grains of magnetite. The speed and flow pattern of the grains were observed with a polarizing microscope while the acoustic intensity through the oil was varied. The pattern will be compared with the light intensity pattern for the nematic liquid crystal in Section III–B. The grains were of the order

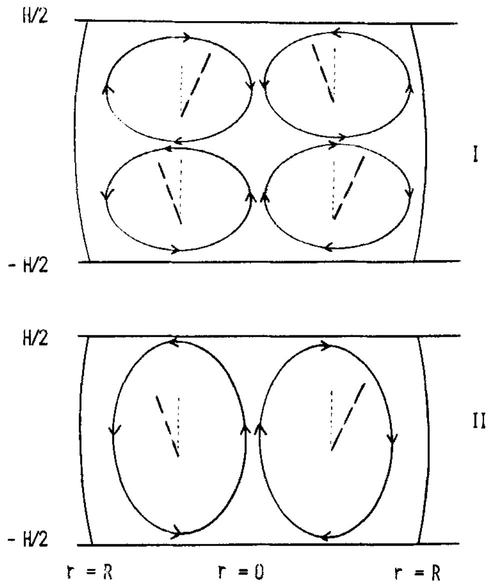

FIGURE 2 Flow patterns in the disc due to acoustic streaming. The upper diagram, I, is the pattern from our second order solutions. The lower pattern, II, is what one may naturally expect since the incident wave approaches normal to the glass surface. The dashed line shows the orientation of the director, tilted from the orientation imposed by the boundaries.

of one micron in diameter. Since the thickness of the disc was 0.032 cm the particle size was small compared to the distance over which the speed of the fluid changed appreciably. The diameter of the disc was from one to four mm, small compared to the 12.7 mm diameter of the barium titanate transducer used to produce the acoustic wave. The microscope was calibrated so the vertical position of the particle whose speed was being measured could be determined when the microscope was focused on that particle.

Using a capillary viscometer the ratio of viscosity to density of the oil was determined, $n/\rho = 0.66 \pm 0.03$ cm^2/sec. From Eq. (14) we see k_0' can now be determined if we know the frequency and wave speed. We take $c = 1.46 \times 10^5$ cm/sec and $f = 0.26$ MHz. We find the real part of $k_0'^2$ small so $k_0' = 1{,}112\,(1 + i)$/cm.

From Eq. (22) we see that the radial flow goes to zero at $r = 0$ due to the $J_1(k_0 r)$ factor. The flow becomes larger for larger values of r and then goes to zero near the edge $r = R$ due to the derivative of $J_1(k_0 r)$. The magnitude of v_{2z} on the other hand is larger at $r = 0$ and decreases as r is increased and finally increases but with a different sign near $r = R$. A diagram of the flows our equations predict is shown in Figure 2–I. If the fluid is observed at $r = R/2$ by focusing the microscope from the top to the bottom of the cell,

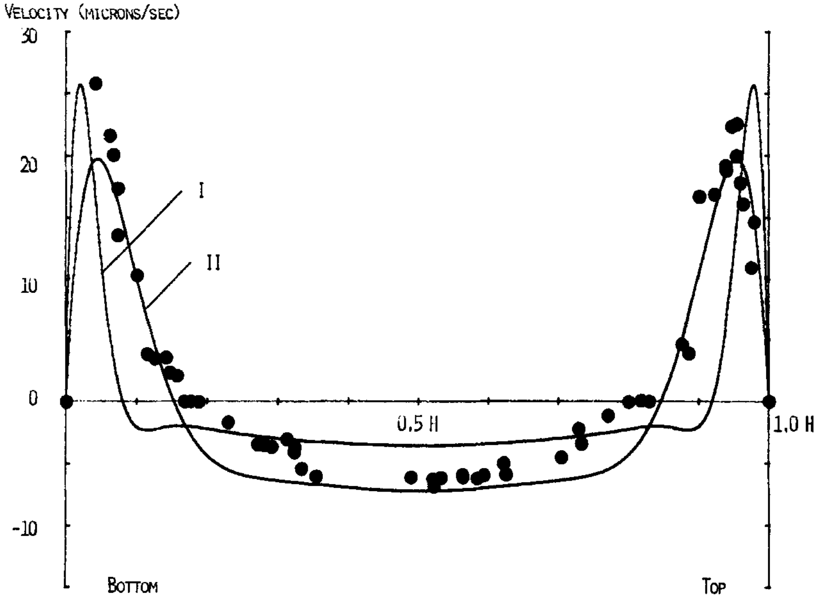

FIGURE 3 Velocity of fluid due to acoustic streaming versus distance through the disc at $r = R/2$. Curve I is a best fit to the data using our measured value of k'_0. Curve II is a best fit allowing k'_0 to be determined by the fitting process itself.

one may see the particles flowing toward the center near the top of the cell, toward the edge near the center ($z = 0$), and again toward the center near the bottom. This is indeed the pattern in Figure 2–I. A more quantitative analysis is presented in Figure 3. The graph shows the fluid speed in the radial direction (toward the center is taken as positive) as a function of z. For the velocity measurements shown in the figure: $R/\lambda = 0.21$ and the frequency is 0.25 MHz. The taller (labelled I) peaked curve in Figure 3 is the best fit of the quantity in brackets in Eq. (22) using our experimentally determined value for k'_0. Since everything in the brackets is determined a best fit was made of the data to a constant times the bracket. The constant thus determined is $(13 \pm 1) \times 10^9$ cm^3 sec/micron and the reduced chi squared we calculate to be $\chi^2 = 2.3$. The smaller peaked curve (labelled II) in Figure 3 is a best fit where both k'_0 and the constant are to be found. Their values are respectively 470 ± 10/cm and $2.0 \pm 0.1 \times 10^9$ cm^3 sec/micron with $\chi^2 = 0.3$. The latter value of k'_0 appears unacceptable in light of the small error in our viscosity experiment and the better fit we take to be fortuitous. It is noteworthy that for both cases the fit is better than one might expect since for the data plotted R/λ is about half of the resonant value for which Eq. (22) was derived. It should be noted that the experimental peak near the top of the disc, i.e. the one on the right in Figure 3, is slightly less than the one on the left. The reason for the difference has to do with our assumption that $v_z = A\exp(i\omega t)$ at both the top and bottom of the disc. Making the boundary condition that $v_z = 0$ at the top decreases the theoretical peak by about 80%. The data seem to be in between these two extremes and it would appear we have taken the better approximation in allowing the upper boundary to move. Data were taken for R/λ equal to 0.21, 0.29, 0.30, 0.39, and 0.45. All of the radial velocity profiles have the same basic pattern as that shown in Figure 3. Frequencies of 0.26, 0.68, 0.77, and 1.07 MHz were used both for direct contact of the sample holder with the barium titanate crystal and with the crystal in a cell so that the wave was propagated through about one cm of water before reaching the sample. All of the flow patterns observed in the microscope using the water cell were radial. For the direct contact case with certain frequencies and locations on the crystal it was possible to induce patterns of either two or four rather circular horizontal flow patterns. The discs became slightly distorted from circular to ellipsoidal in shape for these non-radial patterns. These patterns are assumed to be due to a non-uniform oscillation of the crystal. For these cases the pressure must be assumed to be a function of angle. The solutions are similar to those of the well studied oscillating drumhead.

The radial velocity in Eq. (22) is proportional to A^2, the square of the piston velocity amplitude. This amplitude should be proportional to the voltage applied to the transducer. In Figure 4, therefore, we have plotted the radial velocity measured at a fixed r and z as a function of voltage. The solid line is the fit to a voltage square curve. One should note from the smooth curve that there is no threshold for the flow. What earlier researchers interpreted as a threshold for the onset of the acousto-optic effect is the result of the smoothly varying parameters in Eq. (24) below.

B Liquid crystal analysis

The calculation for a nematic assuming a flow pattern similar to that derived here and shown in Figure 2–I was performed by Sripaipan, Hayes and Fang.[6] For a homeotropically aligned nematic disc they obtain the light intensity through crossed polarizers as

$$I = I_0 \sin^2(2\phi)\sin^2\left(\frac{\delta}{2}\right) \tag{24}$$

where ϕ is the angle between the polarization axis of the incident beam and the projection of the optic axis of the material, δ is the phase difference between the ordinary ray and the extraordinary ray and is proportional to the square of the radial component of the director. The radial component

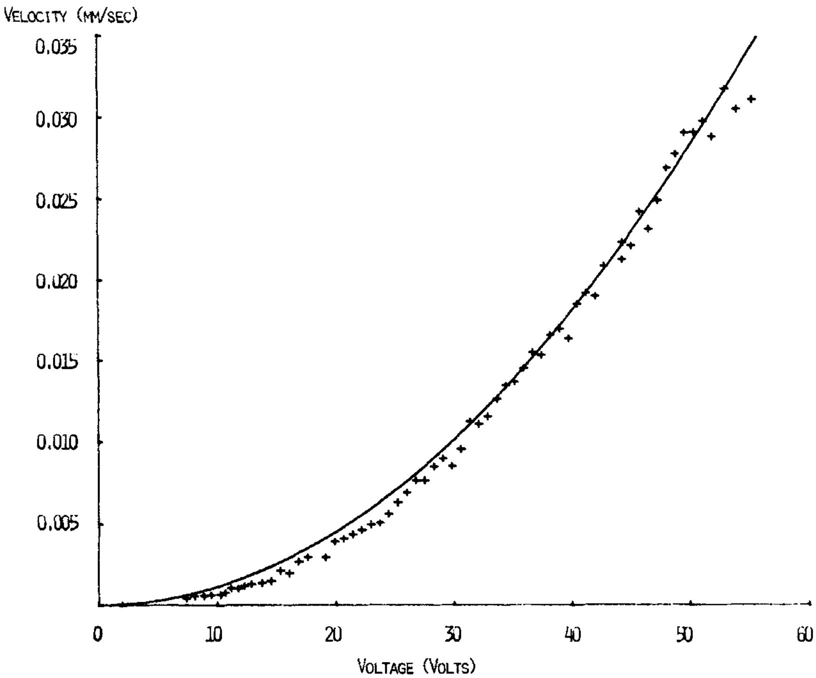

FIGURE 4 Velocity of the fluid due to acoustic streaming versus voltage applied to the transducer. The solid line is the fit to the predicted voltage square dependence.

of the director in turn is proportional to v_{2r}. Therefore, the director splay as shown in Figure 2–I should result in a ring of transmitted intensity for an acoustically excited nematic disc observed with a polarizing microscope. Because of the ϕ dependence in Eq. (24) there should be radial dark bands oriented along the polarization axes. Figure 5 is a series of photomicrographs taken of a nematic disc of 4-cyano-4′-*n*-hexl biphenyl. In Figure 5–A the disc is homeotropically aligned and observed between crossed polarizers. The light transmitted near the circumference is due to surface effects at the nematic air interface. In Figure 5–B the acoustic wave is present and both the predicted white ring and radial bands are visible. For Figure 5–C the acoustic intensity is increased, thereby increasing the director tilt and hence the phase difference, δ, in Eq. (24). Therefore the white ring increases in width and a colored ring appears at $r = R/2$ (shown as a darkened ring in the figure). The colors appear in the correct order for Newton interference colors.

A planar aligned cholesteric disc is similarly studied. The pitch is adjusted by proper mixing of cholesteryl chloride and cholesterol oleyl carbonate so the reflected light is just beyond the visible range, 7000 Angstroms. When the

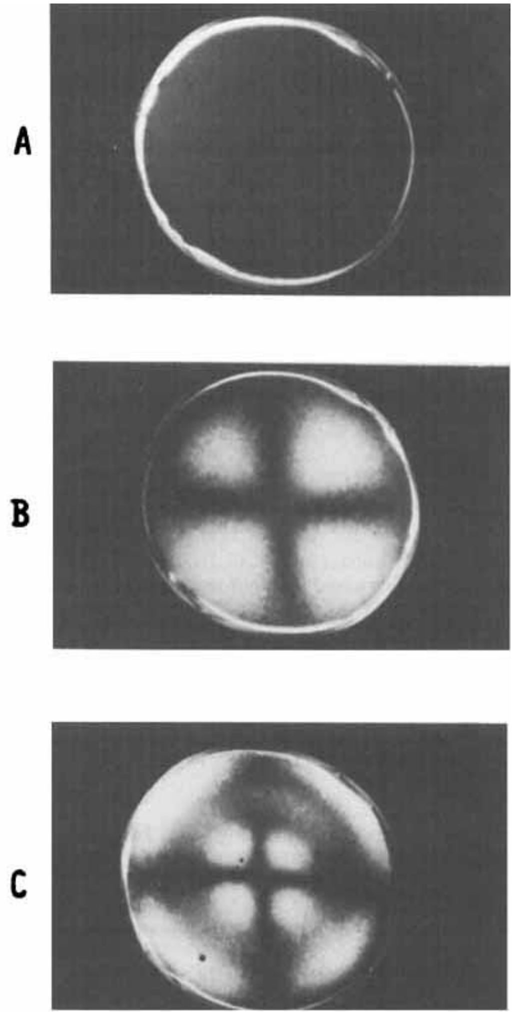

FIGURE 5 Photomicrographs of a nematic disc viewed with a polarizing microscope. In A the nematic is homeotropically aligned with no acoustic wave. In B the acoustic wave is applied. In C the acoustic intensity is increased.

acoustic wave is applied flows develop as described above. The flows turn the pitch axis so that observation is made at an acute angle to the pitch axis. Therefore, the rather dark milky appearance in the planar state changes to a bright multicolored one when the acoustic wave is applied. There are possible device applications to color control by acoustically induced flow in cholesteric liquid crystals.

IV CONCLUSION

We have solved the hydrodynamic equations for an acoustically excited fluid of disc shape to second order in the hydrodynamic variables. We are therefore able to predict explicitly both the magnitude of streaming that should occur and the flow patterns. We experimentally measure the flow and find agreement with the previous predictions, both in for the flow pattern and for the gradual onset of the effect rather than from a threshold.

We conclude that the predominate flow is transverse in agreement with the previous assumptions[6] of earlier work. Finally, observations of an acoustically excited nematic are reported and shown to agree with the predicted pattern. It is felt that these results are the strongest evidence that the acousto-optic effect in liquid crystals is due to streaming and is not a threshold effect.

Acknowledgement

The author wishes to thank P. P. Crooker and W. G. Laidlaw for their many helpful discussions of this work. The research was supported by ONR contract N00014-78-C-0417.

References

1. V. Vzolina and Trudy Lomonosov, *Inst. Akad. Nauk SSSR*, **8**, 11 (1936).
2. L. W. Kessler and S. P. Sawyer, *Appl. Phys. Lett.*, **17**, 440 (1970).
3. W. Helfrich, *Phys. Rev. Lett.*, **29**, 1583 (1972).
4. P. Greguss, *Acustica*, **29**, 52 (1973).
5. J. F. Dreyer, *J. Acoust. Soc. Am.*, **55**, 407 (1974).
6. C. Sripaipan, C. F. Hayes, and G. T. Fang, *Phys. Rev.*, **15A**, 1297 (1977) and C. Sripaipan, C. F. Hayes, and G. T. Fang, *Sixth International Liquid Crystal Conference*, J-29 (1976).
7. S. Nagai, A. Peters, and S. Candau, *Rev. Phys. Appl.* (*Paris*), **12**, 21 (1977), S. Candau and S. Letcher, in *Advances in Liquid Crystals*, Vol. 3, ed. by G. H. Brown (Academic, New York, 1978). S. Candau, A. Peters, and S. Nagai, *Sixth International Liquid Crystal Conference*, J-30 (1976).
8. K. Miyano and Y. R. Shen, *Appl. Phys. Lett.*, **28**, 473 (1976) and *Phys. Rev.*, **A15**, 2471 (1977). *Sixth International Liquid Crystal Conference*, J-31 (1976).
9. J. L. Dion and F. DeForest, *Sixth International Liquid Conference*, K-18 (1976). See also Ref. 11.
10. C. F. Hayes, *Liquid Crystals and Ordered Fluids*, **3**, 287 (1978).
11. J. L. Dion and A. D. Jacob, *Applied Physics Letters*, **31**, 490 (1977).
12. I. A. Chaban, *Sov. Phys. Acoust.*, **24**, 145 (1978).